

# Unsteady mixed convection flow of a micropolar fluid near the stagnation point on a vertical surface

Y.Y. Lok<sup>a</sup>, N. Amin<sup>b</sup>, I. Pop<sup>c,\*</sup>

<sup>a</sup> Center for Academic Services, Kolej Universiti Teknikal Kebangsaan Malaysia, 75450 Ayer Keroh, Melaka, Malaysia

<sup>b</sup> Department of Mathematics, Universiti Teknologi Malaysia, 81310 Johor Bahru, Johor, Malaysia

<sup>c</sup> Faculty of Mathematics, University of Cluj, R-3400 Cluj, CP 253, Romania

Received 6 December 2005; received in revised form 31 January 2006; accepted 31 January 2006

Available online 22 August 2006

## Abstract

The unsteady mixed convection boundary-layer flow of a micropolar fluid near the region of the stagnation point on a double-infinite vertical flat plate is studied. It is assumed that the unsteadiness is caused by the impulsive motion of the free stream velocity and by sudden increase or sudden decrease in the surface temperature from the uniform ambient temperature. The problem is reduced to a system of non-dimensional partial differential equations, which is solved numerically using the Keller-box method. This method may present well-behaved solutions for the transient (small time) solution and those of the steady-state flow (large time) solution. It was found that there is a smooth transition from the small-time solution (initial unsteady-state flow) to the large-time solution (final steady-state flow). Further, it is shown that for both assisting and opposing cases and a fixed value of the Prandtl number, the reduced steady-state skin friction and the steady-state heat transfer from the wall (or Nusselt number) decrease with the increase of the material parameter. On the other hand, it is shown that with the increase of the Prandtl number and a fixed value of the material parameter, the reduced steady-state skin friction decreases when the flow is assisting and it increases when the flow is opposing.

© 2006 Published by Elsevier Masson SAS.

**Keywords:** Mixed convection; Boundary layer; Micropolar fluid; Stagnation point flow

## 1. Introduction

The theory of micropolar fluids has received great attention during the recent years, because the traditional Newtonian fluids cannot precisely describe the characteristic of fluid with suspended particles. Physically micropolar fluids may present the non-Newtonian fluids consisting of dumb-bell molecules or short rigid cylindrical elements, polymer fluids, fluids suspensions and animal blood. The presence of dust or smoke particular in a gas may also be modeled using micropolar fluid dynamics. The theory of micropolar fluids, first proposed by Eringen [1,2], is capable of describing such fluids. In this theory the local effects arising from the microstructure and the intrinsic motion of the fluid elements are taken into account. This is

a kind of continuum mechanics, and many classical flows are being re-examined to determine the effects of fluid microstructure (Willson [3], Bergholz [4], Chandra Shekar et al. [5]). Early studies along these lines may be found in the review article by Peddieson and McNitt [6], and in the recent books by Łukaszewicz [7] and Eringen [8]. Gorla [9], Kumari and Nath [10], and Guram and Smith [11] were the first to apply the micropolar boundary layer theory to problems of steady and unsteady stagnation point flows and claimed that the micropolar fluids model is capable of predicting results which exhibit turbulent flow characteristics, although it is difficult to see how a steady laminar boundary-layer flow could appear to be turbulent. Studies of micropolar fluids have received recently considerable attention due to their applications in a number of processes that occur in industry. Such applications include the extrusion of polymer fluids, solidification of liquid crystals, cooling of a metallic plate in a bath, animal bloods, exotic lubri-

\* Corresponding author.

E-mail address: [pop.ioan@yahoo.co.uk](mailto:pop.ioan@yahoo.co.uk) (I. Pop).

## Nomenclature

$C_f$	local skin friction coefficients
$f$	reduced stream function
$g$	gravitational acceleration ..... $\text{m s}^{-2}$
$Gr$	Grashof number
$h$	reduced microrotation
$j$	microinertia density ..... $\text{m}^2$
$k$	thermal conductivity ..... $\text{W m}^{-1} \text{K}^{-1}$
$K$	dimensionless material parameter
$L$	reference length ..... $\text{m}$
$n$	ratio of the microrotation vector component and the fluid skin friction at the wall
$N$	component of the microrotation vector normal to $x$ – $y$ plane ..... $\text{s}^{-1}$
$Pr$	Prandtl number
$q_w$	heat flux ..... $\text{W m}^{-2}$
$Re$	Reynolds number
$t$	time ..... $\text{s}$
$T$	fluid temperature ..... $\text{K}$
$T_0$	reference temperature ..... $\text{K}$
$u, v$	velocity components along $x$ and $y$ axes ... $\text{m s}^{-1}$
$u_e(x)$	free stream velocity ..... $\text{m s}^{-1}$
$U_e$	reference velocity ..... $\text{m s}^{-1}$

$x, y$  Cartesian coordinates along the wall and normal to it, respectively .....  $\text{m}$

## Greek symbols

$\gamma$	spin gradient viscosity ..... $\text{kg m s}^{-1}$
$\beta$	thermal expansion coefficient ..... $\text{K}^{-1}$
$\eta$	dimensionless transformed variable
$\theta$	dimensionless temperature
$\lambda$	mixed convection parameter
$\kappa$	vortex viscosity ..... $\text{kg m}^{-1} \text{s}^{-1}$
$\mu$	viscosity ..... $\text{kg m}^{-1} \text{s}^{-1}$
$\nu$	kinematic viscosity ..... $\text{m}^2 \text{s}^{-1}$
$\rho$	density ..... $\text{kg m}^{-3}$
$\xi$	dimensionless time

## Subscripts

$e$	boundary-layer edge condition
$w$	wall condition
$\infty$	far field condition

## Superscript

'	differentiation with respect to $\eta$
---	--

cants and colloidal and suspension solutions, for example, for which the classical Navier–Stokes theory is inadequate.

Studies of steady boundary layers of micropolar fluids are many in the open literature. However, there exist relatively fewer studies concerning the unsteady boundary layers of micropolar fluids. Gorla [12] has studied the unsteady mixed convection in micropolar boundary-layer flow over a vertical surface where unsteadiness arises as a result of time-varying nature of the free stream velocity as well as the wall temperature. Also, Gorla et al. [13] have presented an analysis for the unsteady natural convection from a heated vertical surface placed in a micropolar fluid in the presence of internal heat generation or absorption. Therefore, the aim of the present paper is to study the unsteady mixed convection boundary-layer flow of a micropolar fluid near the stagnation point on a heated or cooled vertical surface, where the unsteadiness is caused by the impulsive motion of the free stream velocity  $u_e(x)$  and by sudden increase or sudden decrease in the surface temperature  $T_w(x)$  from the uniform ambient temperature  $T_\infty$ . Only the case when  $T_w(x)$  varies linearly with the distance along the plate,  $x$ , is considered. In such flows with  $T_w(x)$  proportional to  $x$ , the flow and thermal fields are non-symmetric with respect to the stagnation line, see Ramachandran et al. [14]. The short time as well as the long time solutions, i.e. the initial unsteady-state and the final steady-state flows are also included in the analysis. The partial differential equations governing the flow and heat transfer have been solved numerically using an implicit finite-difference scheme known as the Keller-box scheme. An analytical solution has been also obtained for the case of initial unsteady-state flow or small time solution. To the authors' best knowledge this problem has not been studied before. However,

it should be pointed out that the steady combined forced and free convection in the region of a two-dimensional stagnation point on a heated vertical non-isothermal flat plate embedded in a micropolar fluid has been studied recently Hassanien and Gorla [15] and Lok et al. [16]. It has been shown that when  $T_w(x)$  varies linearly with  $x$ , an exact similarity solution exists. Mixed convection in stagnation flows is important when the buoyancy forces, due to the temperature difference between the wall and the free stream, become high and thereby modify the flow and thermal fields significantly. In addition, the local heat transfer rate and local shear stress can be significantly enhanced or diminished in comparison to the pure forced convection case.

## 2. Governing equations

Consider a double-infinite vertical flat plate, which is placed in a micropolar fluid of uniform ambient temperature  $T_\infty$ . It is assumed that at time  $t = 0$  the external flow starts in motion impulsively from rest towards the plate with a steady velocity  $u_e(x)$ . The flow configuration is shown schematically in Fig. 1 together with the corresponding Cartesian coordinates in the vertical and horizontal directions. Either heating or cooling of the plate is assumed to begin simultaneously with the motion of the external stream. It is further assumed that the temperature of the plate  $T_w(x)$  varies linearly with the distance  $x$  along the plate. Therefore, the flow and thermal field are no longer symmetric with respect to the stagnation line about the centerline plane, which contains the stagnation point. Thus, the plate temperature and the condition far from the plate is assumed to be given by

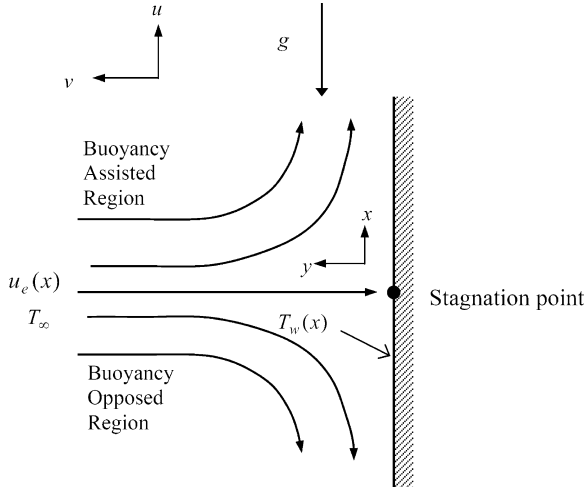


Fig. 1. Physical model and coordinate system.

$$T_w(x) = T_\infty + T_0 \left( \frac{x}{L} \right), \quad u_e(x) = U_e \left( \frac{x}{L} \right) \quad (1)$$

where  $U_e$  is a reference velocity,  $L$  is a characteristic length and  $T_0 > 0$  is a reference temperature. Under these assumptions along with the Boussinesq approximation, the unsteady laminar boundary layer equations governing the mixed convection flow are

$$\frac{\partial u}{\partial x} + \frac{\partial v}{\partial y} = 0 \quad (2)$$

$$\begin{aligned} \frac{\partial u}{\partial t} + u \frac{\partial u}{\partial x} + v \frac{\partial u}{\partial y} \\ = u_e \frac{du_e}{dx} + \left( \frac{\mu + \kappa}{\rho} \right) \frac{\partial^2 u}{\partial y^2} + \frac{\kappa}{\rho} \frac{\partial N}{\partial y} \pm g\beta(T - T_\infty) \end{aligned} \quad (3)$$

$$\rho j \left( \frac{\partial N}{\partial t} + u \frac{\partial N}{\partial x} + v \frac{\partial N}{\partial y} \right) = -\kappa \left( 2N + \frac{\partial u}{\partial y} \right) + \gamma \frac{\partial^2 N}{\partial y^2} \quad (4)$$

$$\frac{\partial T}{\partial t} + u \frac{\partial T}{\partial x} + v \frac{\partial T}{\partial y} = \frac{\nu}{Pr} \frac{\partial^2 T}{\partial y^2} \quad (5)$$

subject to initial and boundary conditions

$$\begin{aligned} t < 0: \quad u(x, y) = v(x, y) = 0, \quad N(x, y) = 0 \\ T(x, y) = T_\infty \quad \text{any } x, y \\ t \geq 0: \quad u(x, 0) = v(x, 0) = 0, \quad x \geq 0 \\ N(x, 0) = -n \frac{\partial u}{\partial y}(x, 0) \\ T(x, 0) = T_w(x) = T_\infty + T_0 \left( \frac{x}{L} \right), \quad x \geq 0 \\ u(x, \infty) = u_e(x) = U_e \left( \frac{x}{L} \right), \quad N(x, \infty) = 0 \\ T(x, \infty) = T_\infty, \quad x \geq 0 \end{aligned} \quad (6)$$

where  $u$  and  $v$  are the velocity components along  $x$  and  $y$  axes,  $N$  is the component of the microrotation vector normal to the  $x$ – $y$  plane,  $T$  is the fluid temperature,  $g$  is the magnitude of the acceleration due to gravity,  $\rho$  is the density,  $\mu$  is the ab-

solute viscosity,  $\kappa$  is the vortex viscosity,  $\gamma$  is the spin-gradient viscosity,  $\nu$  is the kinematic viscosity,  $j$  is the microinertia density,  $Pr$  is the Prandtl number and  $n$  is a constant  $0 \leq n \leq 1$ . It should be mentioned that the case  $n = 0$ , called weak concentration by Guram and Smith [11], which indicates  $N = 0$  near the wall, represents concentrated particle flows in which the microelements close to the wall surface are unable to rotate (Jena and Mathur [17]). The case  $n = 1/2$  indicates the vanishing of anti-symmetric part of the stress tensor and denotes weak concentrations (Ahmadi [18]). The case  $n = 1$ , as suggested by Peddieson [19], is used for the modeling of turbulent boundary layer flows. We shall consider here only the values of  $n = 0$  (weak concentration). It is worth mentioning that we encounter certain difficulties in formulating the problem of boundary layer development due to the impulse motion (see Seshadri et al. [20]). For small time solution (initial unsteady flow) we can use the scale  $y^* = y/(\nu t)^{1/2}$ ,  $t^* = U_e t/x$  and for large-time solution (final steady-state flow) we can use the scale  $\eta = y(U_e/\nu x)^{1/2}$ ,  $t^* = U_e t/x$ . If the problem is formulated in  $(y^*, t^*)$  system, the short-time solution fits in properly, but the large-time solution does not fit. This implies that we have to find a scaling of the  $y$ -coordinate, which behaves like  $y/(\nu t)^{1/2}$  for small time and as  $y(U_e/\nu x)^{1/2}$  for large time. Further, it is convenient to choose a new time scale  $\xi$  so that the region of time integration may become finite. Such transformations have been found by Williams and Rhyne [21], and they are given by

$$\begin{aligned} \eta &= \left( \frac{U_e}{Lv} \right)^{1/2} y \xi^{-1/2}, \quad \xi = 1 - \exp(-t^*), \quad t^* = \left( \frac{U_e}{L} \right) t \\ u(x, y, t) &= U_e \left( \frac{x}{L} \right) f'(\xi, \eta) \\ v(x, y, t) &= - \left( \frac{U_e v}{L} \right)^{1/2} \xi^{1/2} f(\xi, \eta) \\ N(x, \eta, t) &= \left( \frac{U_e}{L} \right) \left( \frac{U_e}{Lv} \right)^{1/2} \left( \frac{x}{L} \right) \xi^{-1/2} h(\xi, \eta) \\ T(x, y, t) &= T_\infty + T_0 \left( \frac{x}{L} \right) \theta(\xi, \eta) \end{aligned} \quad (7)$$

$$\lambda = \frac{Gr}{Re^2}, \quad Gr = \frac{g\beta T_0 L^3}{\nu^2}, \quad Re = \frac{U_e L}{\nu}$$

for  $0 \leq \xi \leq 1$ . Here  $Gr$  is the Grashof number,  $Re$  is the Reynolds number,  $\lambda$  ( $=$  constant) is the mixed convection parameter ( $\lambda > 0$ ) and prime denotes partial differentiation with respect to  $\eta$ . It should be noted that the plus and minus signs in Eq. (3) pertain, respectively, to the buoyancy assisting and the buoyancy opposing flow regions.

We follow the work of many recent authors by assuming that  $\gamma$  is given by, see Rees and Bassom [22] or Rees and Pop [23],

$$\gamma = \left( \mu + \frac{\kappa}{2} \right) j = \mu \left( 1 + \frac{K}{2} \right) j \quad (8)$$

where  $K = \kappa/\mu$  is the material parameter. Using (7) and (8) in Eqs. (2)–(5), we get

$$(1+K)f''' + \frac{1}{2}\eta(1-\xi)f'' + \xi f f'' + \xi(1-f'^2) + Kh' \pm \lambda \xi \theta = \xi(1-\xi) \frac{\partial f'}{\partial \xi} \quad (9)$$

$$\left(1 + \frac{K}{2}\right)h'' + \frac{1}{2}\eta(1-\xi)h' + \xi(fh' - f'h) + \frac{1}{2}(1-\xi)h - K\xi(2h + f'') = \xi(1-\xi) \frac{\partial h}{\partial \xi} \quad (10)$$

$$\frac{1}{Pr}\theta'' + \frac{1}{2}\eta(1-\xi)\theta' + \xi(f\theta' - f'\theta) = \xi(1-\xi) \frac{\partial \theta}{\partial \xi} \quad (11)$$

for  $0 \leq \xi \leq 1$ . The boundary conditions (6) also become

$$\begin{aligned} f(\xi, 0) = f'(\xi, 0) = 0, \quad \theta(\xi, 0) = 1, \\ h(\xi, 0) = -nf''(\xi, 0), \\ f' \rightarrow 1, \quad \theta \rightarrow 0, \quad h \rightarrow 0 \quad \text{as } \eta \rightarrow \infty \end{aligned} \quad (12)$$

for  $0 \leq \xi \leq 1$ . Eqs. (9)–(11) subject to the boundary conditions (12) are coupled non-linear parabolic partial differential equations, but for  $\xi = 0$  ( $t^* = 0$ ) (initial unsteady flow) and  $\xi = 1$  ( $t^* \rightarrow \infty$ ) (final steady-state flow) they reduce to ordinary differential equations.

For  $\xi = 0$  (initial unsteady-state flow), Eqs. (9)–(11) reduce to

$$(1+K)f''' + \frac{1}{2}\eta f'' + Kh' = 0 \quad (13)$$

$$\left(1 + \frac{K}{2}\right)h'' + \frac{1}{2}\eta h' + \frac{1}{2}h = 0 \quad (14)$$

$$\frac{1}{Pr}\theta'' + \frac{1}{2}\eta\theta' = 0 \quad (15)$$

subject to the boundary conditions

$$\begin{aligned} f(0) = f'(0) = 0, \quad \theta(0) = 1, \quad h(0) = -nf''(0) \\ f' \rightarrow 1, \quad \theta \rightarrow 0, \quad h \rightarrow 0 \quad \text{as } \eta \rightarrow \infty \end{aligned} \quad (16)$$

Further, for  $\xi = 1$  (final steady-state flow), Eqs. (9)–(11) become

$$(1+K)f''' + ff'' + 1 - f'^2 + Kh' \pm \lambda \theta = 0 \quad (17)$$

$$\left(1 + \frac{K}{2}\right)h'' + fh' - f'h - K(2h + f'') = 0 \quad (18)$$

$$\frac{1}{Pr}\theta'' + f\theta' - f'\theta = 0 \quad (19)$$

subject to the same boundary conditions (16). It should be noted that for  $K = 0$  (Newtonian fluid) and  $T_w(x)$  varies linearly with  $x$ , Eqs. (17)–(19) reduced to those found by Ramachandran et al. [14].

Eqs. (13)–(15) subject to the boundary conditions (16) admit the closed form solution which is given by

$$\begin{aligned} f'(\eta) = 1 - \operatorname{erfc}\left(\frac{\eta/2}{(1+K)^{1/2}}\right) \\ + 2n\left(\frac{2+K}{2+2K}\right)^{1/2} \left[1 - 2n + 2n\left(\frac{2+K}{2+2K}\right)^{1/2}\right]^{-1} \\ \times \left\{ \operatorname{erfc}\left(\frac{\eta/2}{(1+K)^{1/2}}\right) - \operatorname{erfc}\left[\frac{\eta}{2}\left(\frac{2}{2+K}\right)^{1/2}\right] \right\} \end{aligned} \quad (20)$$

$$\begin{aligned} g(\eta) = -\frac{n}{\sqrt{\pi}}(1+K)^{-1/2} \left[1 - 2n + 2n\left(\frac{2+K}{2+2K}\right)^{1/2}\right]^{-1} \\ \times \exp\left(-\frac{\eta^2}{2(2+K)}\right) \end{aligned} \quad (21)$$

$$\theta(\eta) = \operatorname{erfc}\left(\frac{\eta\sqrt{Pr}}{2}\right) \quad (22)$$

where  $\operatorname{erfc}(\cdot)$  is the complementary error function.

The skin friction coefficient on the surface can be expressed as

$$\begin{aligned} C_f = \frac{x/L}{(1/2)\rho u_e^2(x)} \left\{ (\mu + \kappa) \frac{\partial u}{\partial y} + \kappa N \right\}_{y=0} \\ = 2\xi^{-1/2} Re^{-1/2} \{1 + (1-n)K\} f''(\xi, 0) \end{aligned} \quad (23)$$

for  $0 < \xi \leq 1$ . Similarly, the heat transfer coefficient in terms of the Nusselt number can be written as

$$Nu = \frac{L}{T_w - T_\infty} \left(-\frac{\partial T}{\partial y}\right)_{y=0} = \xi^{-1/2} Re^{1/2} [-\theta'(\xi, 0)] \quad (24)$$

for  $0 < \xi \leq 1$ .

### 3. Results and discussion

The coupled partial differential equations (9)–(11) subject to the boundary conditions (12) as well as the ordinary differential equations (17)–(19) subject to the boundary conditions (16) were solved numerically using a very efficient implicit finite-difference method that is known as the Keller-box method in conjunction with the Newton's linearization technique as described by Cebeci and Bradshaw [24]. It is worth mentioning that this method has been successfully used by the present authors to study the development of the boundary layer flow near the forward and rear stagnation points of a plane surface placed in a micropolar fluid, see Lok et al. [25,26]. Representative results for the velocity, microrotation and temperature profiles, as well as for the skin friction coefficient and Nusselt number have been obtained for  $n = 0$ , and some values of the Prandtl number  $Pr$ , material parameter  $K$  and the mixed convection parameter  $\lambda$ . We shall consider here that  $\lambda = 1$ .

Numerical results representing the values of the reduced steady-state ( $\xi = 1$ ) skin friction coefficient,  $f''(1, 0)$  and the steady-state heat transfer from the wall, or Nusselt number  $Nu/Re^{1/2} = -\theta'(1, 0)$  are given in Tables 1 and 2 for a range values of the Prandtl number  $Pr$  and material parameter  $K$  when the flow is assisting and opposing, respectively. The values found by Ramachandran et al. [14], Hassanien and Gorla [15], and Lok et al. [16] for  $K = 0$  (Newtonian fluid) have also been included in these tables and it is seen that the results are found to be in good agreement. Therefore, it can be concluded that the developed code can be used with great confidence to study the problem discussed in this paper. It is seen from Tables 1 and 2 that when the value of  $Pr$  increases, the steady-state heat transfer from the wall,  $-\theta'(1, 0)$ , increases because fluids with lower thermal conductivity makes the thermal boundary-layer thickness decreases and this lead to an increase in steady-state heat transfer from the wall. However, in the case

Table 1

Values of  $f''(1, 0)$  and  $-\theta'(1, 0)$  for different values of  $K$  and  $n = 0$  for steady-state flow ( $\xi = 1$ ) when the flow is assisting

$Pr$	$K = 0$ (Newtonian fluid)		$K = 1$		$K = 2$		$K = 3$	
	$f''(1, 0)$	$-\theta'(1, 0)$	$f''(1, 0)$	$-\theta'(1, 0)$	$f''(1, 0)$	$-\theta'(1, 0)$	$f''(1, 0)$	$-\theta'(1, 0)$
0.7	1.7064 (1.7063) {1.70632} [1.706376]	0.7641 (0.7641) {0.76406} [0.764087]	1.1346	0.6957	0.8798	0.6568	0.7327	0.6300
7	1.5180 (1.5179) [1.517952]	1.7226 (1.7224) [1.722775]	1.0106	1.5352	0.7849	1.4315	0.6549	1.3621
20	1.4486 (1.4485) [1.448520]	2.4577 (2.4576) [2.458836]	0.9677	2.1807	0.7528	2.0289	0.6290	1.9287
40	1.4102 (1.4101) [1.410094]	3.1023 (3.1011) [3.103703]	0.9443	2.7518	0.7354	2.5624	0.6149	2.4393
60	1.3903 (1.3903) [1.390311]	3.5560 (3.5514) [3.555404]	0.9322	3.1584	0.7264	2.9460	0.6076	2.8095
80	1.3773 (1.3774) [1.377429]	3.9195 (3.9095) [3.914882]	0.9243	3.4874	0.7205	3.2588	0.6028	3.1130
100	1.3677 (1.3680) {1.38471} [1.368070]	4.2289 (4.2116) {4.23372} [4.218462]	0.9186	3.7696	0.7162	3.5286	0.5994	3.3759

( ) Results by Ramachandran et al. [14]; { } Results by Hassanien and Gorla [15]; [ ] Results by Lok et al. [16].

Table 2

Values of  $f''(1, 0)$  and  $-\theta'(1, 0)$  for different values of  $K$  and  $n = 0$  for steady-state flow ( $\xi = 1$ ) when the flow is opposing

$Pr$	$K = 0$ (Newtonian fluid)		$K = 1$		$K = 2$		$K = 3$	
	$f''(1, 0)$	$-\theta'(1, 0)$	$f''(1, 0)$	$-\theta'(1, 0)$	$f''(1, 0)$	$-\theta'(1, 0)$	$f''(1, 0)$	$-\theta'(1, 0)$
0.7	0.6916 (0.6917) {0.69166} [0.691693]	0.6332 (0.6332) {0.63325} [0.633269]	0.5111 [0.511154]	0.5903 [0.590372]	0.4162 [0.416261]	0.5646 [0.564695]	0.3591 [0.359159]	0.5465 [0.546612]
7	0.9234 (0.9235) [0.923528]	1.5457 (1.5403) [1.546374]	0.6595	1.4011	0.5280	1.3179	0.4499	1.2615
20	1.0031 (1.0031) [1.003158]	2.2684 (2.2683) [2.269380]	0.7079	2.0414	0.5638	1.9132	0.4787	1.8282
40	1.0461 (1.0459) [1.045989]	2.9095 (2.9054) [2.907781]	0.7337	2.6141	0.5829	2.4505	0.4940	2.3438
60	1.0680 (1.0677) [1.067703]	3.3636 (3.3527) [3.356338]	0.7468	3.0240	0.5926	2.8386	0.5018	2.7189
80	1.0823 (1.0817) [1.081719]	3.7288 (3.7089) [3.713824]	0.7553	3.3565	0.5989	3.1554	0.5069	3.0266
100	1.0926 (1.0918) {1.11516} [1.091840]	4.0403 (4.0097) {4.04092} [4.015974]	0.7615	3.6421	0.6035	3.4288	0.5105	3.2930

( ) Results by Ramachandran et al. [14]; { } Results by Hassanien and Gorla [15]; [ ] Results by Lok et al. [16].

of buoyancy assisting flow, as the  $Pr$  increases, the reduced steady-state skin friction  $f''(1, 0)$  decreases whereas the opposite trend is observed in the case of buoyancy opposing flows.

The variation of the skin friction coefficient  $2^{-1} Re^{1/2} C_f$  and the Nusselt number  $2^{-1} Re^{-1/2} Nu$  with time  $\xi$  ( $0 < \xi \leq 1$ ) is

shown in Fig. 2 for  $Pr = 7$  and some values of  $K$ . The skin friction coefficient is given by Eq. (23) while we multiply Eq. (24) with  $2^{-1}$  for comparison purposes with the results by Sheshadri et al. [20] for  $K = 0$  (Newtonian fluid). The comparison of the results shows again very good agreement and therefore we are

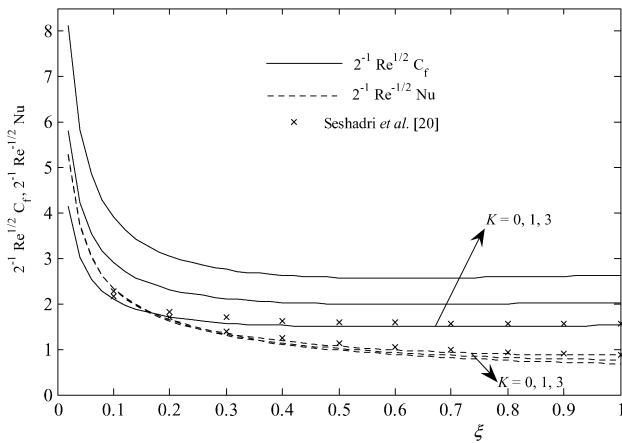


Fig. 2. Variation of the skin friction coefficient ( $2^{-1} Re^{1/2} C_f$ ) and the Nusselt number ( $2^{-1} Re^{1/2} Nu$ ) with time  $\xi$  for  $Pr = 7$  when the flow is assisting.

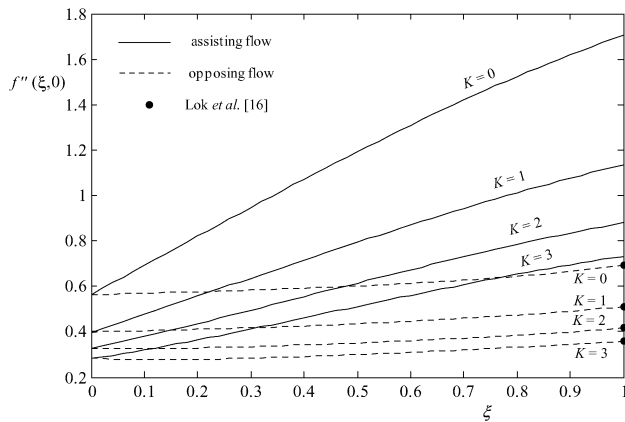


Fig. 3. Variation of the reduced skin friction coefficient  $f''(\xi, 0)$  with time  $\xi$  when  $Pr = 0.7$ .

confident that the present results are accurate. We notice from this figure that at given time (fixed value of  $\xi$ ), the skin friction coefficient increases with  $K$  due to the coefficient  $(1 + K)$  in front of  $f''(\xi, 0)$ , while the Nusselt number decreases with the increase of  $K$ . Therefore, for the present unsteady problem, the micropolar fluids ( $K \neq 0$ ) lead to a decrease of the heat transfer from the wall. On the other hand, it is seen that the skin friction and heat transfer coefficients have large values for small time ( $\xi \ll 0$ ) after the start of the motion and they decrease continuously and reach the steady-state values at  $\xi = 1$ . This is a characteristic property of the impulsive motion, see Telionis [27]. The corresponding results for the buoyancy opposing flow are qualitatively similar to the above results therefore they are not shown here.

Further, the variation with time  $\xi$  ( $0 \leq \xi \leq 1$ ) of the reduced skin friction coefficient  $f''(\xi, 0)$  and the reduced heat transfer from the wall  $-\theta'(\xi, 0)$  are shown in Figs. 3 and 4, respectively for  $Pr = 0.7$  and  $K = 0, 1, 2$  and 3. Meanwhile, Figs. 5 and 6 show the variation of  $f''(\xi, 0)$  and  $-\theta'(\xi, 0)$  with time  $\xi$  ( $0 \leq \xi \leq 1$ ) for some values of  $Pr$ . Results of Ramachandran et al. [14], Lok et al. [16] and Williams and Rhyne [21] for the steady-state flow ( $\xi = 1$ ) have been also shown in these figures.

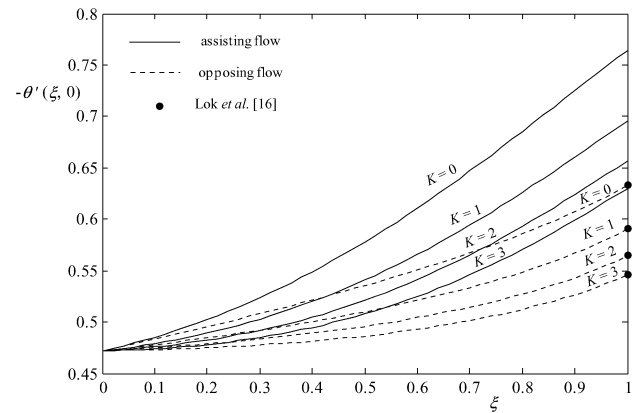


Fig. 4. Variation of the reduced Nusselt number  $-\theta'(\xi, 0)$  with time  $\xi$  when  $Pr = 0.7$ .

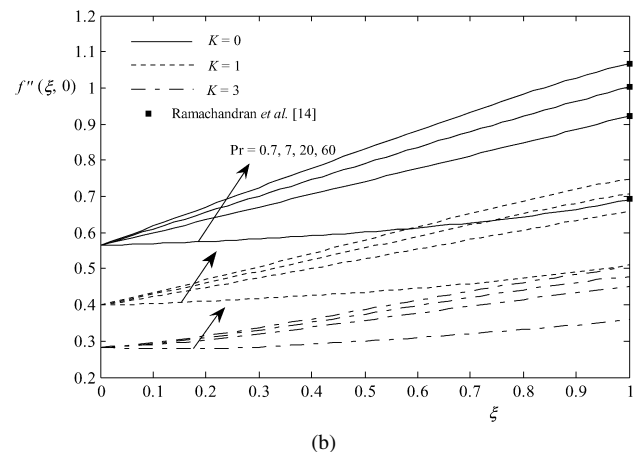
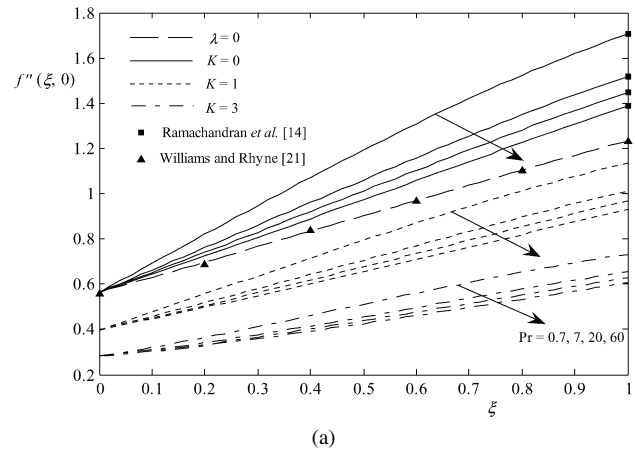


Fig. 5. Variation of the reduced skin friction coefficient with time for some values of  $K$  and  $Pr$ . (a) Assisting flow; (b) Opposing flow.

The results have been found in excellent agreement. It is clearly seen that both  $f''(\xi, 0)$  and  $-\theta'(\xi, 0)$  decrease as  $K$  increase and this is in accordance with the results presented in Tables 1 and 2. It is seen further that, the buoyancy assisting flow cases have a higher value than the buoyancy opposing cases. Fig. 5 shows that for a fixed value of  $Pr$ ,  $f''(\xi, 0)$  increases with the time  $\xi$  ( $0 \leq \xi \leq 1$ ) and this increase is more for the lower  $Pr$

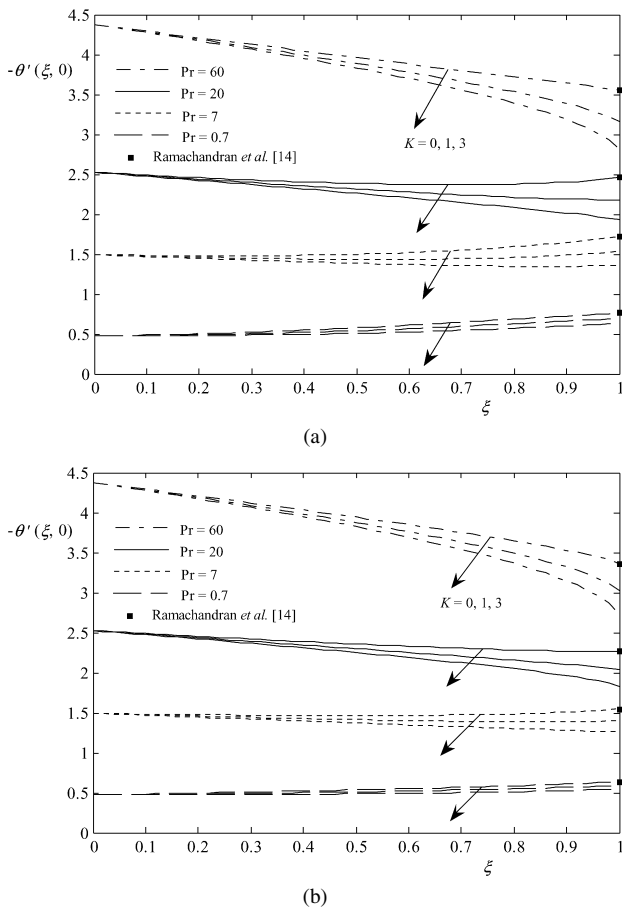


Fig. 6. Variation of the reduced Nusselt number with time for some values of  $K$  and  $Pr$ . (a) Assisting flow; (b) Opposing flow.

when the flow is assisting. However, opposite trend is observed when the flow is opposing where the increase is more for the higher values of  $Pr$ . Profiles in Fig. 6 of the surface heat transfer  $-\theta'(\xi, 0)$  for both assisting and opposing flows show that it changes little with  $\xi$  except when  $Pr$  is large ( $Pr = 60$ ). This is because the higher Prandtl number fluid has a lower thermal conductivity which results in thinner thermal boundary layer and hence a higher heat transfer rate at the surface, as can be seen from Tables 1 and 2. This is in agreement with the results reported by Seshadri et al. [20] for a Newtonian fluid ( $K = 0$ ). Finally, we notice at this place from Figs. 2–6 that there is a smooth transition from the short time solution ( $\xi = 0$ ) to the large time solution ( $\xi = 1$ ).

Figs. 7–9 show the distribution of the velocity  $f'(\xi, \eta)$ , microrotation  $-h(\xi, \eta)$  and temperature  $\theta(\xi, \eta)$  profiles within the boundary layer for  $Pr = 0.7$ ,  $K = 1$  and some values of time  $\xi$  ( $0 \leq \xi \leq 1$ ). Both the buoyancy assisted and opposed cases are considered. It is seen that these profiles develop rapidly as  $\xi$  increases from zero and they attain the steady-state flow at  $\xi = 1$  ( $t^* \rightarrow \infty$ ). It can be also seen that there is a smooth transition from the small time solution to the large time solution. Profiles for other values of the material parameter  $K$  are quite similar with those for  $K = 1$  and for the sake of space limitation these profiles are not shown here.

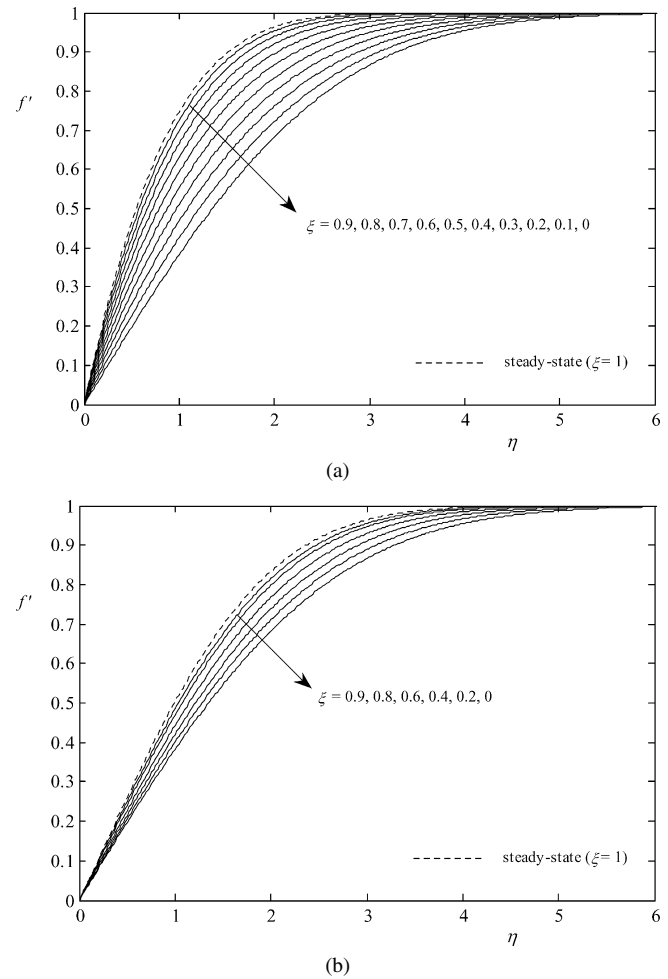


Fig. 7. Velocity profiles for  $K = 1$  and some values of time  $\xi$  and  $Pr = 0.7$ . (a) Assisting flow; (b) Opposing flow.

#### 4. Conclusions

The problem of unsteady mixed convection in two-dimensional stagnation flows of micropolar fluids on a vertical flat plate when the plate temperature  $T_w(x)$  varies linearly with the distance along the plate has been considered in this paper. Both the buoyancy assisting flow (heated surface) and buoyancy opposing flow (cooled surface) situations are considered. The governing non-linear coupled partial differential equations are transformed, using suitable transformations, in a more convenient form for numerical computation. These equations are solved numerically using a very efficient implicit finite-difference scheme, namely the Keller-box method. An analytical solution has been also obtained for the initial unsteady flow or small-time solution ( $\xi = 0$ ). Numerical results for the velocity, temperature and microrotation profiles, as well as the skin friction and Nusselt number are presented in some graphs for various parameter conditions. In addition, the reduced steady-state skin friction and steady-state heat transfer from the plate are given in two tables. It is found that the skin friction and heat transfer, in general, increase with time and there is a smooth transition from the small-time solution (initial unsteady state-flow) to the large-time solution (final steady-state solution).

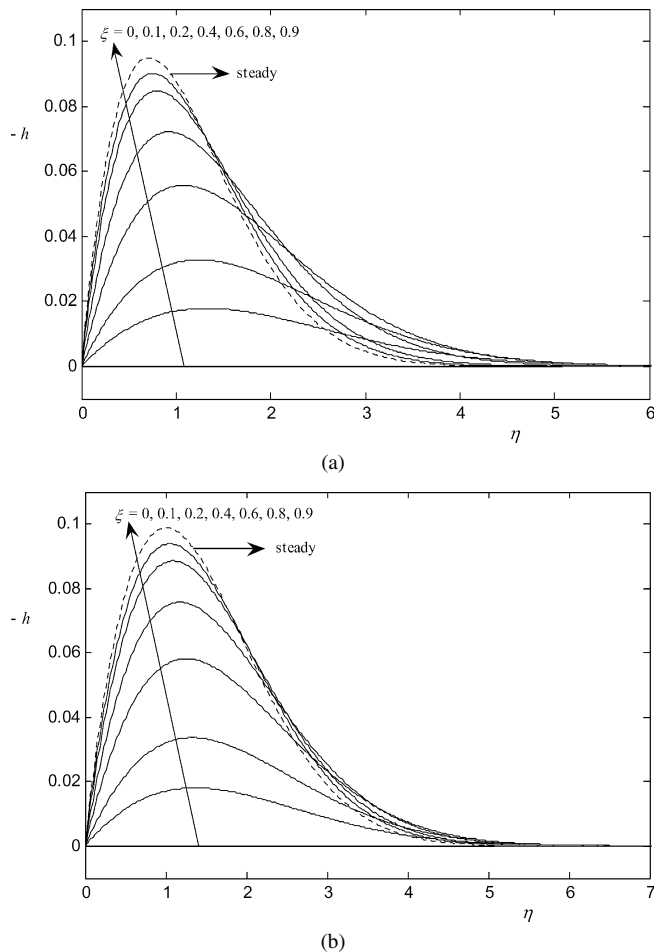


Fig. 8. Microrotation profiles for  $K = 1$  and some values of time  $\xi$  and  $Pr = 0.7$ . (a) Assisting flow; (b) Opposing flow.

## References

- [1] A.C. Eringen, Theory of micropolar fluids, *J. Math. Mech.* 16 (1966) 1–18.
- [2] A.C. Eringen, Theory of thermomicropolar fluids, *J. Math. Anal. Appl.* 38 (1972) 480–496.
- [3] A.J. Willson, Boundary-layer in micropolar liquids, *Proc. Cambridge Philos. Soc.* 67 (1970) 469–476.
- [4] R.F. Bergholz, Natural convection of a heat generating fluid in a closed cavity, *ASME J. Heat Transfer* 102 (1980) 242–247.
- [5] B. Chandra Shekar, P. Vasseur, L. Robillard, T.H. Nguyen, Natural convection in a heat generating fluid bounded by two horizontal concentric cylinders, *Canad. J. Chem. Engrg.* 62 (1984) 482–489.
- [6] J. Peddieson, R.P. McNitt, Boundary layer theory for a micropolar fluid, *Recent Adv. Engrg. Sci.* 5 (1970) 405–476.
- [7] G. Łukasiewicz, *Micropolar Fluids: Theory and Application*, Birkhäuser, Basel, 1999.
- [8] A.C. Eringen, *Microcontinuum Field Theories. II: Fluent Media*, Springer, New York, 2001.
- [9] R.S.R. Gorla, Micropolar boundary layer at a stagnation point, *Int. J. Engrg. Sci.* 21 (1983) 25–34.
- [10] M. Kumari, G. Nath, Unsteady incompressible boundary layer flow of a micropolar fluid at a stagnation point, *Int. J. Engrg. Sci.* 22 (1984) 755–768.
- [11] G.S. Guram, C. Smith, Stagnation flows of micropolar fluids with strong and weak interactions, *Comput. Math. Appl.* 6 (1980) 213–233.
- [12] R.S.R. Gorla, Unsteady mixed convection in micropolar boundary layer flow on a vertical plate, *Fluid Dynam. Res.* 15 (1995) 237–250.

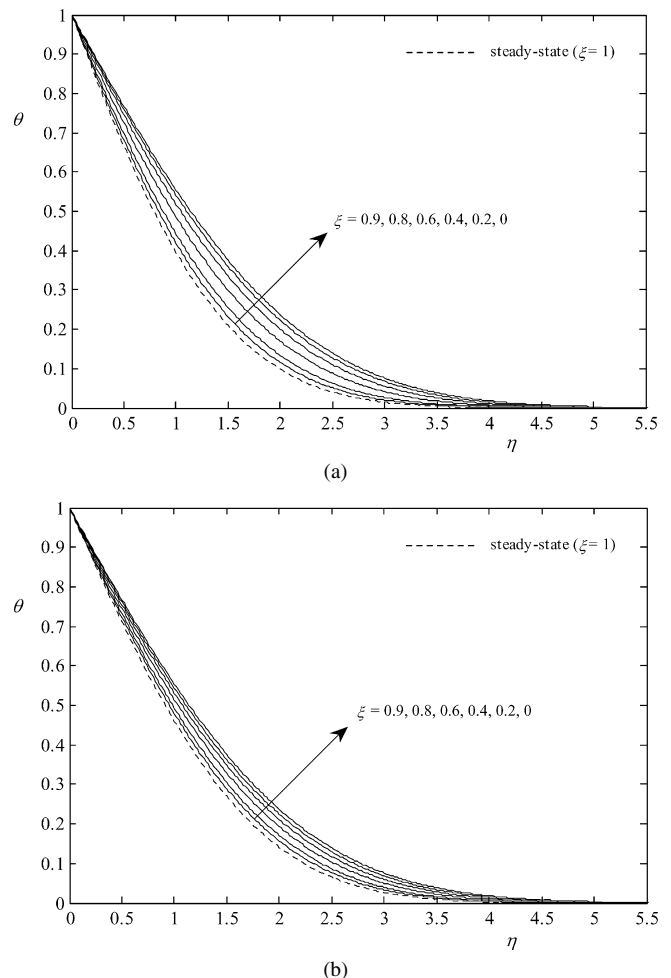


Fig. 9. Temperature profiles for  $K = 1$  and some values of time  $\xi$  and  $Pr = 0.7$ . (a) Assisting flow; (b) Opposing flow.

- [13] R.S.R. Gorla, A.A. Mohammedien, M.A. Mansour, I.A. Hassanien, Unsteady natural convection from a heated vertical plate in micropolar fluid, *Numer. Heat Transfer, Part A* 28 (1995) 253–262.
- [14] N. Ramachandran, T.S. Chen, B.F. Armaly, Mixed convection in stagnation flows adjacent to vertical surfaces, *ASME J. Heat Transfer* 110 (1998) 373–377.
- [15] I.A. Hassanien, R.S.R. Gorla, Combined forced and free convection in stagnation flows of micropolar fluids over vertical non-isothermal surfaces, *Int. J. Engrg. Sci.* 28 (1990) 783–792.
- [16] Y.Y. Lok, N. Amin, D. Campean, I. Pop, Steady mixed convection flow of a micropolar fluid near the stagnation point on a vertical surface, *Int. J. Numer. Methods Heat Fluid Flow* 15 (2005) 654–670.
- [17] S.K. Jena, M.N. Mathur, Similarity solutions for laminar free convection flow of a thermomicropolar fluid past a nonisothermal flat plate, *Int. J. Engrg. Sci.* 19 (1981) 1431–1439.
- [18] G. Ahmadi, Self-similar solution of incompressible micropolar boundary layer flow over a semi-infinite plate, *Int. J. Engrg. Sci.* 14 (1976) 639–646.
- [19] J. Peddieson, An application of the micropolar fluid model to the calculation of turbulent shear flow, *Int. J. Engrg. Sci.* 10 (1972) 23–32.
- [20] R. Seshadri, N. Sreeshylan, G. Nath, Unsteady mixed convection flow in the stagnation region of a heated vertical plate due to impulsive motion, *Int. J. Heat Mass Transfer* 45 (2002) 1345–1352.
- [21] J.C. Williams, T.H. Rhyne, Boundary layer development on a wedge impulsively set into motion, *SIAM J. Appl. Math.* 38 (1980) 215–224.
- [22] D.A.S. Rees, A.P. Bassom, The Blasius boundary-layer flow of a micropolar fluid, *Int. J. Engrg. Sci.* 34 (1996) 113–124.
- [23] D.A.S. Rees, I. Pop, Free convection boundary-layer flow of a micropolar fluid from a vertical flat plate, *IMA J. Appl. Math.* 61 (1998) 179–197.



- [24] T. Cebeci, P. Bradshaw, *Physical and Computational Aspect of Convective Heat Transfer*, Springer, New York, 1984.
- [25] Y.Y. Lok, P. Phang, N. Amin, I. Pop, Unsteady boundary layer flow of a micropolar fluid near the forward stagnation point of a plane surface, *Int. J. Engrg. Sci.* 41 (2003) 173–186.
- [26] Y.Y. Lok, N. Amin, I. Pop, Unsteady boundary layer flow of a micropolar fluid near the rear stagnation point of a plane surface, *Int. J. Thermal Sci.* 42 (2003) 995–1001.
- [27] D.P. Telionis, *Unsteady Viscous Flows*, Springer, New York, 1981.